Computers and Concrete, *Vol. 23, No. 1 (2019) 1-10*
DOI: https://doi.org/10.12989/cac.2019.23.1.001

Seismic investigation of pushover methods for concrete piers of curved bridges in plan

Hamid Reza Ahmadi[∗1], Nariman Namdari[2a], Maosen Cao[3b] and Mahmoud Bayat[4c]

[1]Department of Civil Engineering, Faculty of Engineering, University of Maragheh, Maragheh, P.O. Box 55136-553, Iran
[2]Department of Civil Engineering, Bandar Abbas Branch, Islamic Azad University, Bandar Abbas, Iran
[3]Department of Engineering Mechanics, Hohai University, 210098 Nanjing, Jiangsu, People's Republic of China
[4]Department of Civil and Environmental Engineering, University of Pittsburgh,
3700 O'Hara Street, 729 Benedum Hall, Pittsburgh, PA 15261, USA

(Received October 10, 2018, Revised December 23, 2018, Accepted December 30, 2018)

Abstract. The use of non-linear analysis of structures in a functional way for evaluating the structural seismic behavior has attracted the attention of the engineering community in recent years. The most commonly used functional method for analysis is a non-linear static method known as the "pushover method". In this study, for the first time, a cyclic pushover analysis with different loading protocols was used for seismic investigation of curved bridges. The finite element model of 8-span curved bridges in plan created by the ZEUS-NL software was used for evaluating different pushover methods. In order to identify the optimal loading protocol for use in astatic non-linear cyclic analysis of curved bridges, four loading protocols (suggested by valid references) were used. Along with cyclic analysis, conventional analysis as well as adaptive pushover analysis, with proven capabilities in seismic evaluation of buildings and bridges, have been studied. The non-linear incremental dynamic analysis (IDA) method has been used to examine and compare the results of pushover analyses. To conduct IDA, the time history of 20 far-field earthquake records was used and the 50% fractile values of the demand given the ground motion intensity were computed. After analysis, the base shear vs displacement at the top of the piers were drawn. Obtained graphs represented the ability of a cyclic pushover analysis to estimate seismic capacity of the concrete piers of curved bridges. Based on results, the cyclic pushover method with ISO loading protocol provided better results for evaluating the seismic investigation of concrete piers of curved bridges in plan.

Keywords: curved bridges; pushover analysis; cyclic loading; incremental dynamic analysis

1. Introduction

The use of non-linear static analysis, called pushover analysis, dates back to 1970. Over the next 10 to 15 years, numerous articles were published on this method. The main focus of these researches was the scope of application, advantages and disadvantages of the pushover analysis, and its comparison with linear and non-linear dynamic methods. All proposed methods for performance-based design used non-linear static analysis to find the capacity curve. The purpose of pushover analysis was to evaluate the performance of a structure by estimating resistance and deformation capacities through on-liner static analysis, and then comparing these capacities with demands at equal levels of performance (Bozorgnia, and Bertero 2004). Pushover analysis was identified in the past few years and used in seismic instructions (Antoniou and Pinho 2004a). Since determinant information based on the response obtained from linear methods (static or dynamic) was not achieved, this pushover method also had limitations such as the inability to consider higher modes or severe drops in stiffness. These problems were associated with approximations for structures, especially in irregular structures and in general structures with higher modes that have indescribable effects (Krawinkler and Seneviratna 1998).

Due to the capability of the method, various procedures of this method have been widely used and evaluated by researchers (Mahdavi *et al*. 2012, Panyakapo 2014, Jeon *et al*. 2015, Bayat *et al*. 2017a, b, 2015, Faal and Poursha 2017, Sobhan *et al*. 2017, Luo *et al*. 2017, Naghadehi 2011, 2016, 2017, Hashemi *et al*. 2015, 2014, 2018, Alkayem *et al*. 2018, Kia *et al*. 2018).

A significant number of curved bridges are built and serviced around the world. For example, horizontally curved bridges form a significant part of the bridge population in the United States, so, one-third of the steel bridges made in the United States are curved (DeSantiago *et al*. 2005, Amiri Hormozaki*et al*. 2015). Many of these bridges need retrofitting for various reasons including design and construction based on old codes, increasing years of operation, and increasing traffic loads. Therefore, their seismic capacity must be properly estimated; hence, it is necessary to use analytical methods that have low computational costs with high precision.

∗Corresponding author, Assistant Professor
E-mail: ahmadi@maragheh.ac.ir
[a]E-mail: nariman.namdari@gmail.com
[b]E-mail: cmszhy@163.com
[c]E-mail: mbayat14@yahoo.com

http://www.techno-press.org/?journal=cac&subpage=8 ISSN: 1598-8198 (Print), 1598-818X (Online)

In general, the pushover method is one of the most important methods for evaluating the capacity of bridges. However, the accuracy of different pushover procedures in the calculation of capacity curves is different. Over the past few years, a cyclic pushover analysis method has been used to evaluate seismic behavior of building frames. Results indicated the ability of this method to investigate seismic performance of buildings. In this research, for the first time, a cyclic pushover analysis was used to evaluate seismic behavior of curved bridges along with conventional pushover and adaptive pushover methods. Additionally, the optimal lateral loading protocol for cyclic pushover was identified. To evaluate the results, this analysis was compared to IDA. The time history of 20 far-source earthquake records was used to conduct the IDA.

2. Pushovermethods

2.1.Conventional pushover

This method is presented in different codes such as SEAOC (1995), ATC40 (1996), FEMA273 (1997), FEMA356 (2000), and EC8 (2005). In this method, the specific loading pattern is selected and the lateral load intensity increases uniformly, which is usually done with uniform or triangular distribution of lateral loads. The crack sequence, plastic hinges, and structural failure are determined by this method. The loading continues till the target displacement is reached or the structure is destroyed. Target displacement is used to express the maximum movement, which is similar to the displacement of the structure due to the expected earthquake. Considering the constraints of the conventional method, many efforts have been made to improve it. Different methods have been suggested by various researchers including the adaptive pushover analysis method (Antoniou and Pinho 2004b).

Advanced pushover analysis has been proposed by researchers in various approaches. In these approaches, researchers have attempted to consider the higher mode effects. Additionally, they have tried to propose methods in which the distribution of the lateral load at each level is proportionate to the strength and stiffness variation of the structure. The force-based and displacement-based adaptive pushover are of the most important adaptive pushover methods. Regarding the advantages of displacement-based adaptive pushover, it is used in this research.

2.2 Displacement-based adaptive pushover method

The adaptive pushover method consists of four steps: a) Definition of nominal load vector and mass inertia; b) Calculation of load factor; c) Calculation of normalized size vector; and d) Upgrading of displacement vector. In this method, the displacement in each step of the analysis is obtained by the following equation

$$u = \lambda . u_0 \tag{1}$$

In this equation, λ is the load factor and is determined by the force control algorithm; and $u_0$is a numerical vector.

To determine the load vector form (or increase the load vector) at each stage and before increasing the load, the vector of the normalized scale is calculated by the following equation using the Lanczos algorithm

$$D_i = \sqrt{\sum_{j=1}^{n} D_{ij}^2} = \sqrt{\sum_{j=1}^{n} (\Gamma_j \varphi_j)^2} \tag{2}$$

$$\overline{D}_i = \frac{D_i}{\max D_i} \tag{3}$$

In this equation, I is the story number; j is the mode number; Γ_j is the modal participation coefficient of the j^{th} mode; and φ_{ij} is the mass normalized mode shapes for the i^{th} story and j^{th} mode. Finally, the vector of load u_t in step t^{th} is calculated by the following equation

$$U_t = U_{t-1} + \Delta_t \overline{D}_t + u_o \tag{4}$$

In this equation, $\Delta\lambda_t$ is the increased load factor; U_{t-1} is the load vector in the previous step; andu_0 is the initial nominal load vector value.

2.3 Cyclic pushover method

The cyclic pushover method is among other promising procedures. This is a relatively new procedure for assessing seismic behavior of structures. In general, this method depends on the analysis of the modal response of non-linear structures. The dynamic equation of the single degree of freedom (SDOF) system under the influence of the seismic load is as follows (Chopra 2016)

$$\ddot{D}_n + 2\zeta_n \omega_n \dot{D}_n + \frac{F_{sn}}{L_n} = -\ddot{u}_g(t) \tag{5}$$

In this equation, D_n, $\dot{D}_n$, $\ddot{D}_n$ are the terms of displacement, velocity, and modal acceleration, respectively; and ξ_n, ω_n are modal damping and modal angular frequency, respectively. The internal resisting modal force is calculated from the relationship $F_{sn} = \{\phi_n\}^T \left\{f_s(D_n, \dot{D}_n)\right\}$. In addition, $L_n = \{\phi_n\}^T [m]\{i\}$ where $\{\phi_n\}$, $[m]$ and $\{i\}$ are modal shape vector, mass matrix and the unit vector, respectively. In addition, $\ddot{u}_g(t)$ is the ground motion acceleration.

In order to solve this equation, application of the analysis of dynamic time history is a common solution. Of course, the relationship between F_{sn} and D_n can also be obtained with a pushover analysis. In a modal pushover analysis, the lateral force distribution in the pushover analysis in any mode is f_n, which is obtained by the following equation

$$f_n = \Gamma_n [m]\{\phi_n\} A_n \tag{6}$$

$$A_n = \omega_n^2 D_n \tag{7}$$

The modal participation factor is calculated as follows

$$\Gamma_n = \frac{L_n}{M_n} = \frac{\{\phi_n\}^T [m]\{i\}}{\{\phi_n\}^T [m]\{\phi_n\}} \tag{8}$$

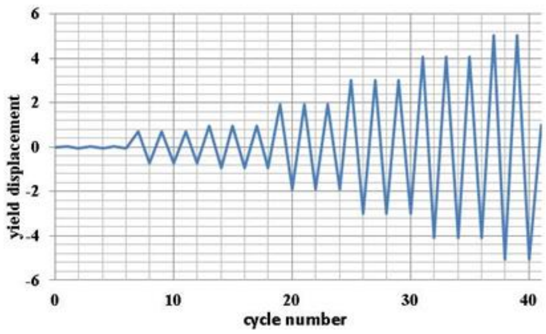

Fig. 1 Loading Protocol ATC-24

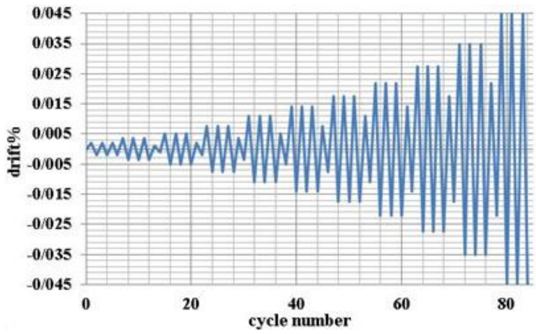

Fig. 3 Loading Protocol FEMA461

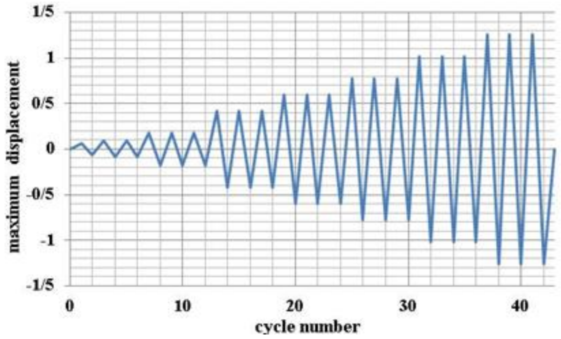

Fig. 2 Loading Protocol ISO

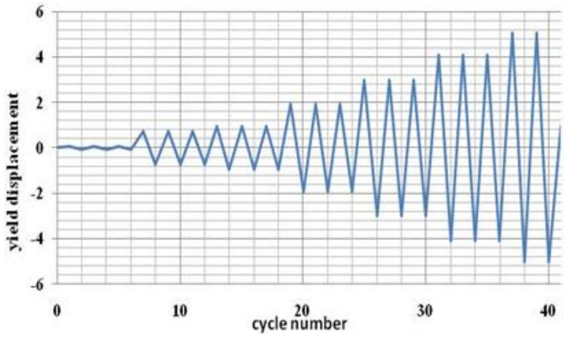

Fig. 4 Loading Protocol ACI

Where M_n is normalized modal mass of nth mode. In the cyclic pushover analysis, lateral force distribution in each mode is defined as follows

$$f_n^* = \lambda_i \Gamma_n [m]\{\phi_n\} A_n \qquad (9)$$

In this equation, λ_i is the variability factor that determines the direction of the force and is defined as follows: if I is an odd number, then λ_i=1; and if I is an even number, then λ_i=−1. The structure is subjected to the load distribution in a positive direction, so that the displacement of the structure reaches the maximum level. Then, force distribution is applied in the negative direction to the structure and continues until maximum displacement. This process is followed by a predetermined time history (Chou and Chen 2011, Anastasopoulos *et al*. 2012, Gidaris and Taflanidis 2013, Purba and Bruneau 2015, Oinam *et al*. 2017). In structures which higher modes effects on structural responses, these influences are considered using cyclic pushover analysis.

In order to understand the importance of pushover analysis in seismic evaluation of structures and due to the multiplicity of different procedures in the pushover method, this research has used a number of pushover methods including conventional, adaptive, and cyclic. Conventional and adaptive methods have been previously used to evaluate seismic behavior of bridges. Considering the importance of curved bridges in plan and the necessity of seismic study of these structures through analytical methods (that have good computational costs at high precision), a cyclic pushover analysis was used in this research, for the first time, to evaluate the seismic behavior of curved bridges. One of the most important factors in a cyclic pushover analysis is the loading protocol.

In order to identify the optimal loading protocol for use in a static non-linear cyclic analysis of curved bridges, four loading protocols were suggested by valid references including ISO (2007), ATC-24 (Krawinkler 1992), FEMA461 (2007), and ACI (2005). The diagrams for loading protocols are shown in Figs. 1-4.

3. Introducing the curved bridge

In this research, a bridge was studied by considering all members of its structure including the deck, the piers connections between deck and piers and connections between deck and abutments. The structure was modeled by Burdette *et al*. (2008a) in the Zeus-NL software (2010). The geometry and configuration of the bridge, the height of the piers, the modeling of the elements, and the cross section of the elements are shown in Figs. 5-9.

The bridge was 344 meters long with nine spans and eight piers, and its concrete deck is made up of prestressed box sections. The first and end spans of the bridge were 32 meters long, and the mid-spans had a length of 40 meters. The bridge piers are single-column with circular cross section. The radius of curvature of the deck is 200 meters. The connection of the piers and abutements to the foundations is also considered rigid support. To Model the connection of the deck to the piers and abutements, springs with linear and nonlinear behavior were used. Besides, beam element which its nonlinear behavior is considered by using fiber elements, were used to model the piers and decks. Mass modeling was considered centrally in the nodes related to the deck elements and at the top of the piers. Two different behavioral model were used to model the concrete behavior. The Mander model (1988) is used in monotonic

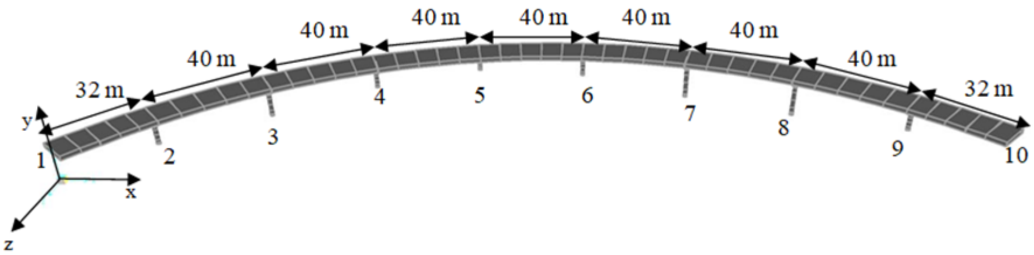

Fig. 5 Geometry of the bridge along with number of piers and span length

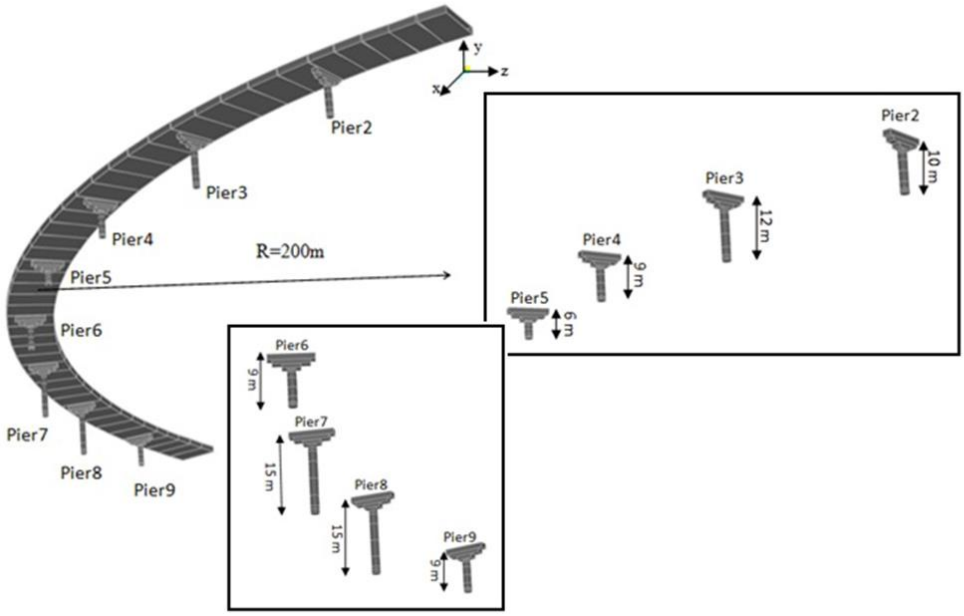

Fig. 6 Bridge configuration to be studied in a 3D space with heights of piers

Table 1 Comparison of the bridge model period

Mode number	Period of reference (Burdette *et al*. 2008a)	Period of analysis
1	0.938	0.94
2	0.677	0.68
3	0.545	0.54
4	0.46	0.46

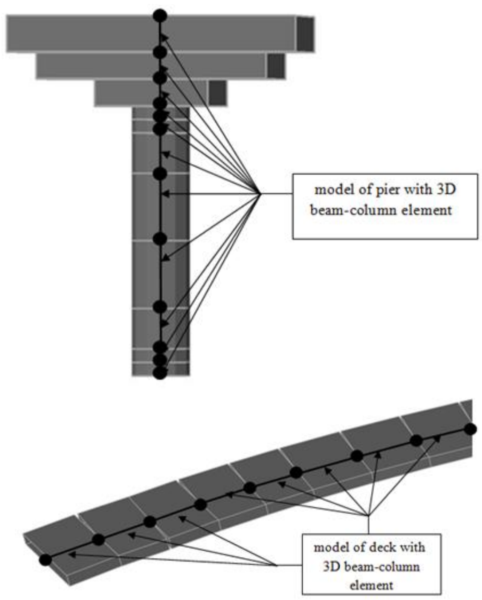

Fig. 7 Modeling the deck, piers, and beam-column

modes. The expanded model by Rueda and Elnashai (Martínez-Rueda and Elnashai 1997) which are able to consider the reduction of hardness and strength under cyclic loads with numerical stability, were used in the cyclic modes.

The behavior of steel in reinforced concrete was modeled by bilinear elasto-plastic behavior. In order to ensure the performance of the bridge model, results of the analysis were compared with the results presented in references (Burdette *et al*. 2008a). Based on the comparison, the analytical model responses are very close to the reference results. The first four modes of the structure are shown in the Table 1.

4. Analysis and assessment of results

4.1 Determination of the critical pier

In this study, various loading protocols have been used for the cyclic pushover analysis. In some of these protocols, it was necessary to determine the bridge pier that yielded object displacement. For this purpose, the conventional pushover analysis was performed and yielding displacement

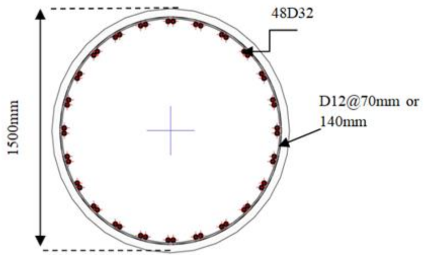

Fig. 8 Cross section of piers

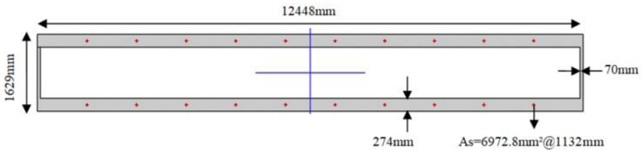

Fig. 9 Cross section of deck

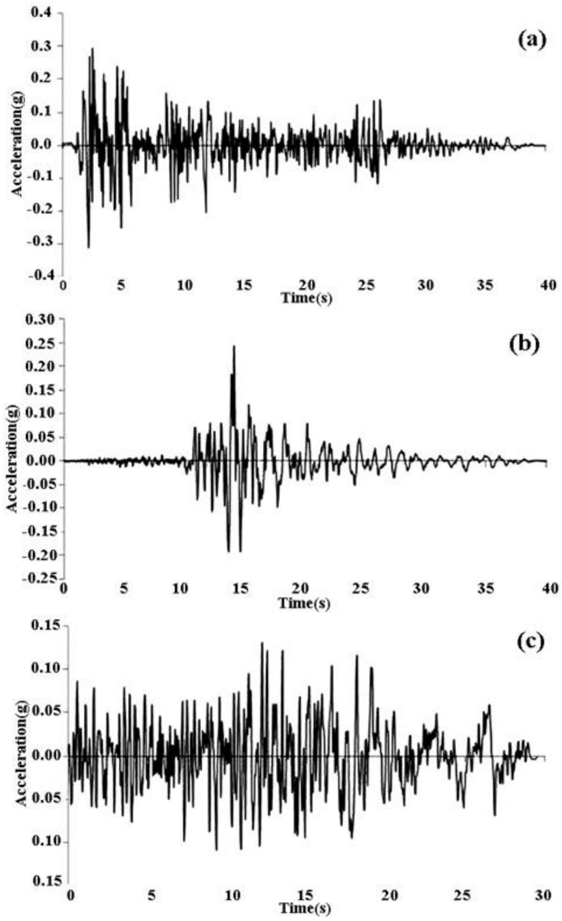

Fig. 10 Acceleration time histories of the earthquakes (a) El Centro, (b)Loma Prieta and (c) Manjil

was calculated for each pier. In some other protocols, it was necessary to calculate the maximum displacement of piers and, accordingly, determine the loading protocol. Due to the height difference among piers, displacement corresponding to the pier yield (D_y) and their maximum displacement (D_m) were different. However, it was necessary to identify critical piers, and calculate the displacement of D_y and D_m.

In order to determine the critical piers and their maximum displacement, acceleration time histories of

Table 2 Displacement capacity at the tops of bridge piers

Pier number	2	3	4	5	6	7	8	9
Displacement capacity(mm)	358	500	295	145	295	757	757	295

Table 3 Specification of records used in IDA

row	Earthquake name	Year of the event	Station of registration	Magnitude	PGA	*R* (km)
1	Bam	2003	Cheshmehsabz	6.6	0.0234	191
2	Borah peak	1983	Reactor Plant	6.88	0.0335	100
3	ChiChi	1999	CHY022	5.9	0.0104	106
4	Dinar	1995	Bardar	6.4	0.0165	36
5	Friuli	1976	Barcis	6.5	0.0292	49
6	Georjia	1991	Oni	6.2	0.0754	42
7	Kozani	1995	Edessa	6.4	0.0232	75
8	Landers	1992	Mel Canyon	7.28	0.0296	126
9	Luma Prita	1992	Death Valley	5.65	0.068	98
10	Manjil	1990	Tehran	7.37	0.0165	175
11	Morgan Hill	1984	San Juanto Dam	6.19	0.0793	32
12	Norcia	1979	Bevagna	5.9	0.0235	31
13	Northridge	1994	Anacapa Island	6.69	0.0673	66
14	N. Palm Springs	1986	Puerta La Cruz	6.06	0.0767	67
15	Parkfield	1966	San Louis	6.19	0.0118	63
16	Pelekanada	1984	Pelekanada	5.0	0.1735	155
17	San fernando	1971	Springs Pumphouse	6.61	0.0270	92
18	Tabas	1978	Bajestan	7.35	0.0907	120
19	Taiwan	1983	SMART1 E02	6.5	0.0056	92
20	Whittier Narrows	1987	Castaic - Hasley Canyon	5.99	0.0316	63

ElCentro, Loma Prieta, and Manjil earthquakes were applied to the bridge, and a non-linear dynamic analysis was carried out with different scales. Diagrams of the time histories are displayed in Fig. 10. Maximum displacement values of pier vertices were recorded in the transverse direction at each step. Earthquake intensity was increased by multiplying a scalar quantity as a scale factor to the acceleration time history of each earthquake. For one of the piers, an increase in earthquake intensity continued to the point where top displacement of the pier reached its displacement capacity. The scale factor corresponding to the displacement capacity of the pier is considered as the scale of ultimate capacity and the pier is identified as the critical pier, too. Rayleigh damping has been used in time history analysis. Caltrans (2010) relationship has also been used to determine displacement capacity at the tops of bridge piers. The amount of displacement capacity at the tops of bridge piers was calculated according to regulations; results are shown in Table 2.

By conducting similar analyses for the Loma Prieta and Manjil earthquakes, results of the IDA were also investigated and identified; when maximum displacement at the top of pier 5 reached its displacement capacity, the other piers still showed linear behavior. Therefore, in the Loma Prieta and Manjil earthquakes, pier 5 was the critical pier;

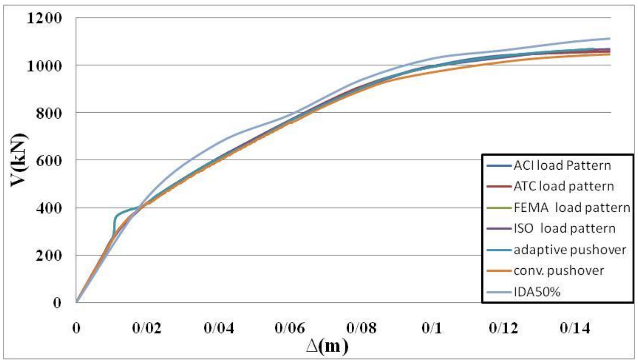

Fig. 11 Pushover and IDA diagrams for pier 2

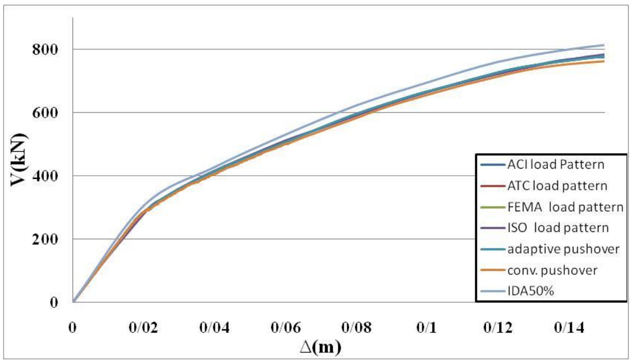

Fig. 12 Pushover and IDA diagrams for pier 3

Table 4 The base shear vs. drift ratio of the top of the pier2

Conv. Pushover		Adaptive Pushover		ACI Load Pattern		ATC Load Pattern		FEMA Load Pattern		ISO Load Pattern		IDA 50%	
drift ratio	*V* (kN)	drift ratio	*V* (kN)	drift ratio	*V* (kN)	drift ratio	*V* (kN)	drift ratio	*V* (kN)	drift ratio	*V* (kN)	drift ratio	*V* (kN)
0.0000	0	0.0000	0	0.0000	0	0.0000	0	0.0000	0	0.0000	0	0.0000	0
0.0007	173	0.0010	259	0.0007	186	0.0008	211	0.0010	259	0.0007	180	0.0010	222
0.0019	405	0.0019	412	0.0017	390	0.0018	395	0.0019	412	0.0018	395	0.0030	558
0.0020	425	0.0022	447	0.0030	517	0.0023	451	0.0022	447	0.0026	480	0.0040	672
0.0042	626	0.0038	589	0.0065	807	0.0042	625	0.0038	589	0.0043	631	0.0060	793
0.0062	786	0.0051	687	0.0083	924	0.0061	773	0.0051	687	0.0071	847	0.0070	865
0.0079	906	0.0061	775	0.0089	952	0.0079	902	0.0061	775	0.0091	964	0.0080	937
0.0091	964	0.0086	939	0.0092	965	0.0094	975	0.0086	939	0.0099	994	0.0100	1028
0.0138	1060	0.0125	1048	0.0122	1043	0.0124	1044	0.0125	1048	0.0119	1031	0.0140	1100
0.0145	1063	0.0145	1070	0.0145	1053	0.0145	1056	0.0145	1070	0.0145	1072	0.0145	1107

Table 5 The base shear vs. drift ratio of the top of the pier3

Conv. Pushover		Adaptive Pushover		ACI Load Pattern		ATC Load Pattern		FEMA Load Pattern		ISO Load Pattern		IDA 50%	
drift ratio	*V* (kN)	drift ratio	*V* (kN)	drift ratio	*V* (kN)	drift ratio	*V* (kN)	drift ratio	*V* (kN)	drift ratio	*V* (kN)	drift ratio	*V* (kN)
0.0000	0	0.0000	0	0.0000	0	0.0000	0	0.0000	0	0.0000	0	0.0000	0
0.0008	142	0.0007	120	0.0007	123	0.0007	120	0.0007	120	0.0006	115	0.0008	153
0.0016	270	0.0021	325	0.0017	292	0.0017	288	0.0015	262	0.0021	331	0.0025	367
0.0020	316	0.0025	361	0.0019	305	0.0025	361	0.0017	288	0.0028	383	0.0033	429
0.0035	422	0.0050	510	0.0032	406	0.0050	510	0.0035	426	0.0050	511	0.0050	531
0.0043	470	0.0066	590	0.0047	494	0.0066	590	0.0066	590	0.0059	554	0.0058	333
0.0057	546	0.0079	649	0.0069	605	0.0079	649	0.0079	649	0.0079	648	0.0067	623
0.0096	714	0.0096	711	0.0092	695	0.0096	711	0.0096	711	0.0103	729	0.0100	760
0.0115	768	0.0107	747	0.0115	765	0.0107	747	0.0107	747	0.0110	749	0.0117	801
0.0121	772	0.0121	771	0.0121	770	0.0121	771	0.0121	771	0.0121	776	0.0121	811

maximum earthquake acceleration corresponding to the final capacity was 0.61 gravity acceleration for the Loma Prieta earthquake and 0.39 gravity acceleration for the Manjil earthquake.

4.2 Perform incremental dynamic analysis

For estimating pushover analysis, a non-linear IDA (Vamvatsikos and Cornell 2002, Bayat *et al*. 2015) was carried out. In fact, pushover analysis results were compared to IDA results, and the ones closest to the IDA were identified as superior pushovers.

According to Table 3, 20 far-field records received (Bayat *et al.* 2017b) from the PEER site (Next Generation Attenuation of Ground Motions 2006) have been used in this study for the IDA (Vamvatsikos and Cornell 2004).

Under the influence of the 20 introduced records, the IDA for the bridge was carried out (as shown in the table above) and IDA curves were calculated. According to the number of graphs obtained for optimum use of calculations, 50% fractile IDA curve which is also called the median IDA, was calculated for each of the piers. The IDA analysis provides an insight of structure behavior.

4.3 Perform pushover analysis

Pushover analysis results along with the median IDA curve are presented in Figs. 11 to 18 and Tables 4-11. In the figures, the vertical axis represents the base shear, and the horizontal axis represents the displacement of the top of the pier. In addition, the base shear vs. drift ratio of the top of the pier is shown in the tables. Each of the proposed analyses will have a more favorable performance if their results are closer to IDA.

In pier 2, the cyclic pushover analysis provided similar results. As shown in Fig. 11, in the capacity curve of the adaptive pushover analysis, a hump was suddenly seen at the end of the linear region, which didnot conform to IDA results. Therefore, the performance of cyclic pushover methods was better than adaptive pushover analysis. Conventional pushover in the linear region showed good performance, but structural capacity was less than estimated in the non-linear region. There was no significant difference in capacity curves generated by various cyclic pushover protocols; however, the ISO protocol is closer to the IDA diagram.

Based on results obtained in pier 3, all pushover analyses exhibited relatively similar performances. The capacity of pier 3 was slightly more in anon-linear dynamic analysis than in static analyses (see Fig. 12 and Table 5).

In pier 4, the difference between results of pushover methods was more evident. According to the results displayed in Fig. 13, the cyclic pushover analysis with ACI loading protocol and conventional pushover analysis did not show satisfactory performance. The other pushover analytical methods in the linear region showed similar results through IDA. At the start of the non-linear area, the IDA showed more capacity for pier 4 as compared to pushover analyses. By evaluating the results, the cyclic pushover analysis with ISO loading protocol provided a

Table 6 The base shear vs. drift ratio of the top of the pier4

Conv. Pushover		Adaptive Pushover		ACI Load Pattern		ATC Load Pattern		FEMA Load Pattern		ISO Load Pattern		IDA 50%	
drift ratio	*V* (kN)	drift ratio	*V* (kN)	drift ratio	*V* (kN)	drift ratio	*V* (kN)	drift ratio	*V* (kN)	drift ratio	*V* (kN)	drift ratio	*V* (kN)
0.0000	0	0.0000	0	0.0000	0	0.0000	0	0.0000	0	0.0000	0	0.0000	0
0.0016	461	0.0014	481	0.0043	772	0.0014	473	0.0014	481	0.0012	426	0.0022	736
0.0019	500	0.0018	583	0.0063	970	0.0026	708	0.0018	583	0.0020	570	0.0033	856
0.0025	575	0.0026	704	0.0072	1040	0.0037	811	0.0026	704	0.0028	726	0.0044	976
0.0055	895	0.0039	829	0.0079	1082	0.0053	989	0.0039	829	0.0047	919	0.0067	1146
0.0076	1065	0.0054	1006	0.0092	1132	0.0070	1122	0.0054	1006	0.0062	1078	0.0089	1187
0.0101	1157	0.0068	1098	0.0102	1162	0.0087	1160	0.0068	1098	0.0079	1140	0.0111	1195
0.0127	1181	0.0076	1146	0.0128	1183	0.0107	1167	0.0076	1146	0.0115	1180	0.0133	1223
0.0154	1199	0.0131	1174	0.0144	1196	0.0138	1213	0.0141	1574	0.0149	1187	0.0156	1228
0.0161	1198	0.0161	1189	0.0161	1198	0.0161	1185	0.0161	1189	0.0161	1190	0.0161	1226

Table 7 The base shear vs. drift ratio of the top of the pier5

Conv. Pushover		Adaptive Pushover		ACI Load Pattern		ATC Load Pattern		FEMA Load Pattern		ISO Load Pattern		IDA 50%	
drift ratio	*V* (kN)	drift ratio	*V* (kN)	drift ratio	*V* (kN)	drift ratio	*V* (kN)	drift ratio	*V* (kN)	drift ratio	*V* (kN)	drift ratio	*V* (kN)
0.0000	0	0.0000	0	0.0000	0	0.0000	0	0.0000	0	0.0000	0	0.0000	0
0.0019	966	0.0041	1539	0.0034	1383	0.0041	1539	0.0041	1539	0.0043	1684	0.0017	726
0.0026	1166	0.0050	1732	0.0049	1716	0.0050	1732	0.0050	1732	0.0057	1848	0.0033	1452
0.0042	1555	0.0055	1801	0.0055	1805	0.0055	1801	0.0055	1801	0.0071	1944	0.0067	1991
0.0068	1923	0.0070	1940	0.0065	1895	0.0070	1940	0.0070	1940	0.0086	2008	0.0100	2103
0.0101	2030	0.0086	2008	0.0074	1959	0.0086	2008	0.0086	2008	0.0100	2046	0.0133	2126
0.0151	2079	0.0131	2057	0.0094	2034	0.0131	2057	0.0131	2057	0.0179	2096	0.0167	2133
0.0191	2130	0.0157	2084	0.0163	2069	0.0157	2084	0.0157	2084	0.0200	2118	0.0200	2109
0.0230	2166	0.0206	2129	0.0210	2130	0.0206	2129	0.0206	2129	0.0233	2153	0.0233	2163
0.0242	2174	0.0242	2157	0.0242	2119	0.0242	2157	0.0242	2157	0.0242	2158	0.0242	2177

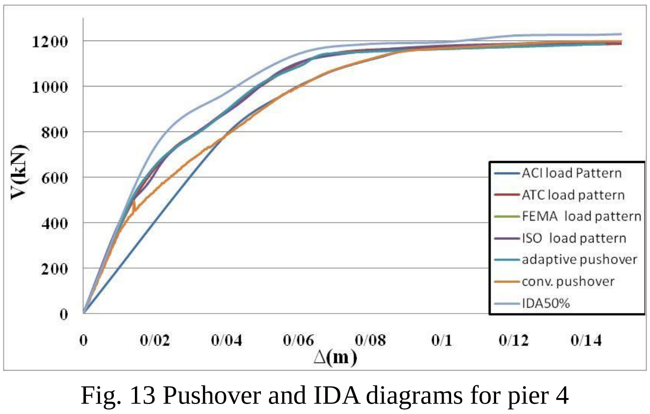

Fig. 13 Pushover and IDA diagrams for pier 4

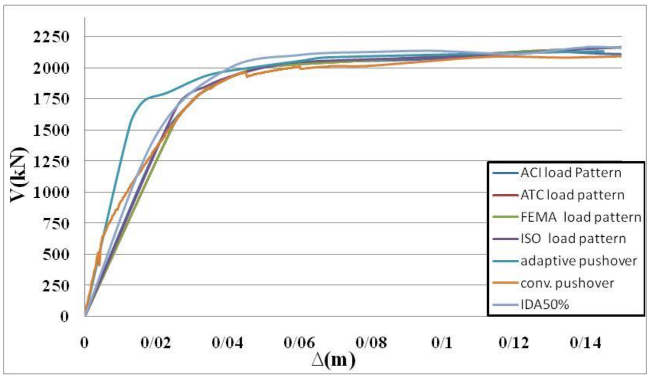

Fig. 14 Pushover and IDA diagrams for pier 5

Table 8 The base shear vs. drift ratio of the top of the pier6

Conv. Pushover		Adaptive Pushover		ACI Load Pattern		ATC Load Pattern		FEMA Load Pattern		ISO Load Pattern		IDA 50%	
drift ratio	*V* (kN)	drift ratio	*V* (kN)	drift ratio	*V* (kN)	drift ratio	*V* (kN)	drift ratio	*V* (kN)	drift ratio	*V* (kN)	drift ratio	*V* (kN)
0.0000	0	0.0000	0	0.0000	0	0.0000	0	0.0000	0	0.0000	0	0.0000	0
0.0010	337	0.0010	398	0.0020	439	0.0016	517	0.0010	398	0.0006	219	0.0022	718
0.0012	382	0.0014	482	0.0029	577	0.0017	633	0.0014	482	0.0012	520	0.0033	852
0.0019	507	0.0020	600	0.0033	672	0.0026	711	0.0020	600	0.0018	612	0.0044	985
0.0028	620	0.0028	694	0.0049	840	0.0037	815	0.0028	694	0.0026	688	0.0067	1147
0.0037	719	0.0039	831	0.0063	969	0.0053	992	0.0039	831	0.0038	822	0.0089	1198
0.0101	1163	0.0040	869	0.0079	1086	0.0070	1128	0.0040	869	0.0062	1082	0.0111	1227
0.0127	1177	0.0049	931	0.0112	1185	0.0087	1167	0.0049	931	0.0079	1146	0.0133	1243
0.0154	1209	0.0106	1142	0.0140	1215	0.0117	1191	0.0106	1142	0.0132	1201	0.0156	1265
0.0161	1214	0.0161	1221	0.0161	1211	0.0161	1222	0.0161	1221	0.0161	1224	0.0161	1269

Table 9 The base shear vs. drift ratio of the top of the pier7

Conv. Pushover		Adaptive Pushover		ACI Load Pattern		ATC Load Pattern		FEMA Load Pattern		ISO Load Pattern		IDA 50%	
drift ratio	*V* (kN)	drift ratio	*V* (kN)	drift ratio	*V* (kN)	drift ratio	*V* (kN)	drift ratio	*V* (kN)	drift ratio	*V* (kN)	drift ratio	*V* (kN)
0.0000	0	0.0000	0	0.0000	0	0.0000	0	0.0000	0	0.0000	0	0.0000	0
0.0009	99	0.0010	113	0.0014	152	0.0010	113	0.0010	113	0.0012	132	0.0013	143
0.0015	169	0.0015	167	0.0020	213	0.0015	167	0.0015	167	0.0017	189	0.0020	194
0.0033	280	0.0017	183	0.0026	249	0.0017	183	0.0017	183	0.0023	232	0.0027	246
0.0045	328	0.0020	216	0.0030	267	0.0022	228	0.0020	216	0.0028	262	0.0040	317
0.0053	351	0.0028	260	0.0043	320	0.0028	261	0.0028	260	0.0040	310	0.0053	357
0.0060	375	0.0040	310	0.0055	358	0.0040	310	0.0040	310	0.0057	364	0.0067	399
0.0076	423	0.0063	382	0.0075	390	0.0063	382	0.0063	382	0.0061	375	0.0080	450
0.0092	468	0.0083	439	0.0092	448	0.0086	447	0.0083	439	0.0069	398	0.0093	480
0.0097	478	0.0097	478	0.0097	465	0.0097	478	0.0097	478	0.0097	481	0.0097	484

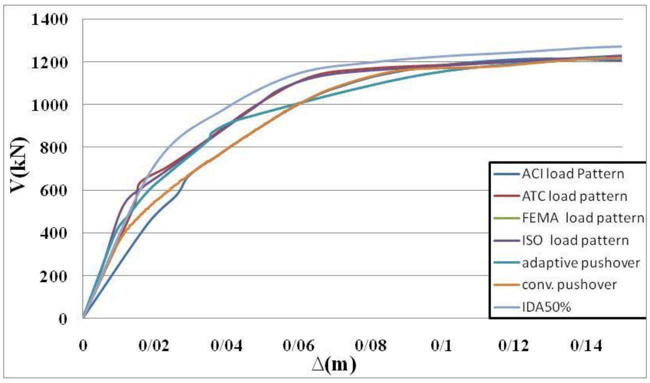

Fig. 15 Pushover and IDA diagrams for pier 6

slightly better capacity curve than the other pushover analyses.

As shown in Fig. 14, the adaptive pushover analysis demonstrated a higher capacity than the IDA in the linear region and in the early non-linear region. However, in comparison with other cyclic pushover analyses, IDA estimated a higher capacity for pier 5. In pier 6, the curve obtained through a cyclic pushover analysis with ACI loading protocol as well as through a conventional pushover had a significant distance from the IDA curve, and did not show satisfactory performance (see Fig. 15). The performances of adaptive and conventional pushover analyses with FEMA loading protocol were close to each

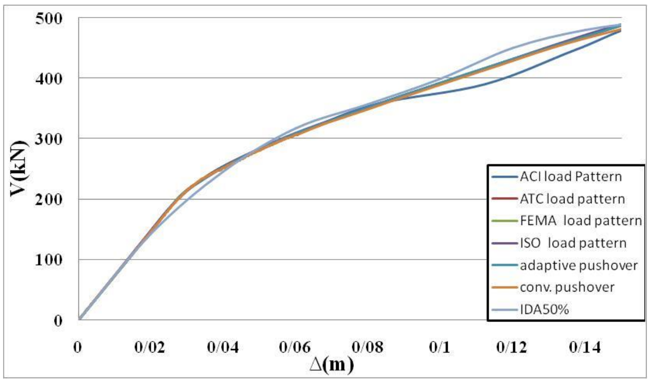

Fig. 16 Pushover and IDA diagrams for pier 7

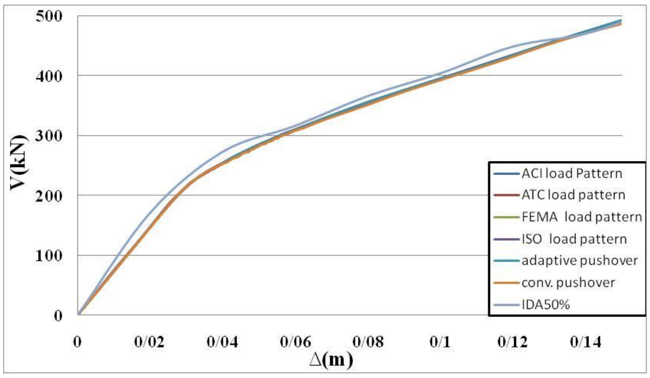

Fig. 17 Pushover and IDA diagrams for pier 8

Table 10 The base shear vs. drift ratio of the top of the pier8

Conv. Pushover		Adaptive Pushover		ACI Load Pattern		ATC Load Pattern		FEMA Load Pattern		ISO Load Pattern		IDA 50%	
drift ratio	*V* (kN)	drift ratio	*V* (kN)	drift ratio	*V* (kN)	drift ratio	*V* (kN)	drift ratio	*V* (kN)	drift ratio	*V* (kN)	drift ratio	*V* (kN)
0.0000	0	0.0000	0	0.0000	0	0.0000	0	0.0000	0	0.0000	0	0.0000	0
0.0007	82	0.0015	167	0.0014	152	0.0010	113	0.0015	167	0.0007	79	0.0013	171
0.0011	123	0.0020	217	0.0017	192	0.0017	184	0.0020	217	0.0012	132	0.0020	222
0.0019	203	0.0022	229	0.0022	230	0.0020	217	0.0022	229	0.0017	189	0.0027	273
0.0037	301	0.0028	261	0.0026	250	0.0022	229	0.0028	261	0.0028	263	0.0040	316
0.0053	353	0.0034	288	0.0030	269	0.0034	288	0.0034	288	0.0034	288	0.0053	366
0.0060	378	0.0052	353	0.0038	302	0.0052	353	0.0052	353	0.0047	334	0.0067	405
0.0076	425	0.0073	415	0.0043	322	0.0073	415	0.0073	415	0.0057	367	0.0080	449
0.0092	472	0.0086	452	0.0055	361	0.0086	452	0.0086	452	0.0071	410	0.0093	470
0.0097	483	0.0097	484	0.0097	448	0.0097	484	0.0097	484	0.0097	484	0.0097	480

other, and both estimated pier capacity better than cyclic pushover analysis with ACI loading protocol; but compared to the cyclic pushover with ISO and ATC loading protocols, they had a greater distance from the non-linear dynamic curve. In pier 6, the performance of cyclic pushover with ISO and ATC loading protocols were better than other pushover analyses.

In piers 7 and 8, the pushover analysis estimated less pier capacity than the non-linear IDA. Based on the calculated results shown in Figs. 16 and 17, in these piers, the pushover analysis showed a similar function; only in pier 7, the cyclic pushover analysis with ACI loading protocol in the non-linear region showed a weaker performance.

Based on results shown in Fig. 18, the cyclic pushover

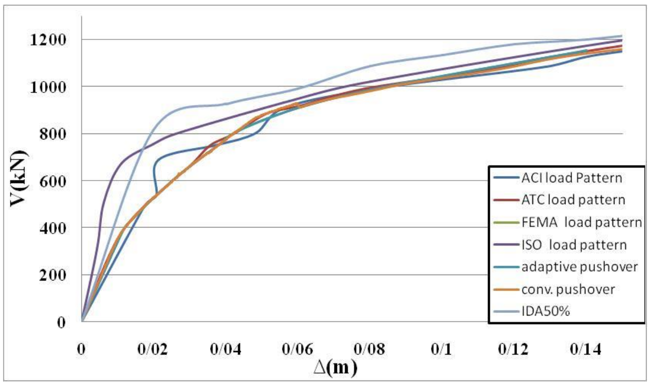

Fig. 18 Pushover and IDA diagrams for pier 9

Table 11 The base shear vs. drift ratio of the top of the pier9

Conv. Pushover		Adaptive Pushover		ACI Load Pattern		ATC Load Pattern		FEMA Load Pattern		ISO Load Pattern		IDA 50%	
drift ratio	*V* (kN)	drift ratio	*V* (kN)	drift ratio	*V* (kN)	drift ratio	*V* (kN)	drift ratio	*V* (kN)	drift ratio	*V* (kN)	drift ratio	*V* (kN)
0.0000	0	0.0000	0	0.0000	0	0.0000	0	0.0000	0	0.0000	0	0.0000	0
0.0012	368	0.0013	387	0.0019	490	0.0012	368	0.0013	387	0.0005	309	0.0022	816
0.0035	683	0.0021	518	0.0024	690	0.0034	662	0.0030	622	0.0007	507	0.0033	871
0.0052	850	0.0030	622	0.0042	752	0.0047	799	0.0035	675	0.0012	672	0.0044	926
0.0067	912	0.0035	675	0.0054	803	0.0057	884	0.0042	748	0.0022	756	0.0067	992
0.0088	978	0.0042	748	0.0063	910	0.0067	919	0.0049	816	0.0029	800	0.0089	1087
0.0101	1015	0.0049	816	0.0092	995	0.0087	992	0.0068	916	0.0062	930	0.0111	1134
0.0127	1070	0.0068	916	0.0143	1085	0.0122	1065	0.0095	1004	0.0089	1022	0.0133	1179
0.0154	1137	0.0095	1004	0.0160	1137	0.0144	1124	0.0133	1044	0.0124	1060	0.0156	1200
0.0161	1149	0.0161	1169	0.0161	1139	0.0161	1162	0.0161	1169	0.0161	1185	0.0161	1208

analysis with ISO protocol in the linear region and in the early non-linear region provided more pier capacity than IDA. However, compared to other pushover analyses, the cyclic pushover analysis with ISO protocol showed better performance.

5. Conclusions

Regarding the number of curve bridges in plan in all of the world and their susceptibility to earthquakes, the seismic investigation of curve bridges in plan in this research is investigated. Pushover analysis is a very powerful technique and is widely used in seismic evaluation of structures. Therefore, various methods of pushover analysis have been presented. In recent years, the cyclic pushover method has been proposed by researchers to evaluate seismic performance of buildings. Considering cyclic pushover analysis specification and multiplicity of loading protocols, cyclic pushover analysis with different protocols was used in this research to study the seismic performance of curved bridges in plan; the optimal loading protocol was also identified in order to evaluate this analytical method for curved bridges. For this purpose, results of static non-linear analyses including cyclic pushover analysis with ACI loading protocol, cyclic pushover analysis with ATC loading protocol, cyclic pushover analysis with FEMA loading protocol, cyclic pushover analysis with ISO loading protocol, conventional pushover analysis and, displacement-based adaptive pushover analysis were compared with that of non-linear IDA.

The analytical model previously studied by Burdette *et al*. (2008b) was used to evaluate the curved bridge in plan. The finite element model of the bridge provided in ZEUS-NL software was evaluated and its reliability was assured. The curved bridge had 8 piers. Pushover analyses were performed along with the IDA. To conduct the IDA, the time history of 20 earthquake records was used, which was eventually plotted with statistical computations of 50%.The base shear displacement of the tops of piers was drawn for the different piers and the performance of each pushover method was compared to non-linear IDA.

Generally speaking, based on the results of this study, cyclic pushover analysis provides better results for evaluating the performance of concrete piers of curved bridges as compared to conventional pushover analysis and also adaptive pushover analysis. This can be due to the reciprocal nature of cyclic pushover analysis which is closer to real behaviour. Among the four protocols, the ISO loading protocol provided better results for evaluating seismic performance of concrete piers of curve bridges in plan. Therefore, according to this research, using cyclic pushover analysis with ISO loading protocol an lead to a better evaluation of seismic performance of concrete piers of curved bridges and somewhat, improve the weaknesses of other pushover methods.

Acknowledgements

"This work is partially supported by International Science and technology cooperation project (Grant no.: BZ2018022)".

References

ACI (2005), Acceptance Criteria for Moment Frames Based on Structural Testing, ACI, USA.

Alkayem, N.F., Cao, M., Zhang, Y., Bayat, M. and Su, Z. (2018), "Structural damage detection using finite element model updating with evolutionary algorithms: a survey", *Neur. Comput. Appl.*, **30**(2), 389-411

AmiriHormozaki, E., Pekcan, G. and Itani, A. (2015), "Analytical fragility functions for horizontally curved steel I-girder highway bridges", *Earthq. Spectra*, **31**(4), 2235-2254.

Anastasopoulos, I., Kourkoulis, R., Gelagoti, F. and Papadopoulos, E. (2012), "Rocking response of SDOF systems on shallow improved sand: An experimental study", *Soil Dyn. Earthq. Eng.*, **40**, 15-33.

Antoniou, S. and Pinho, R. (2004a), "Advantages and limitations of adaptive and non-adaptive force-based pushover procedures", *J. Earthq. Eng.*, **8**(4), 497-522.

Antoniou, S. and Pinho, R. (2004b), "Development and verification of a displacement-based adaptive pushover procedure", *J. Earthq. Eng.*, **8**(5), 643-661.

ATC, A. (1996), 40, Seismic Evaluation and Retrofit of Concrete Buildings, Applied Technology Council, Report ATC-40, Redwood City, USA.

Bayat, M., Daneshjoo, F. and Nisticò, N. (2015), "A novel proficient and sufficient intensity measure for probabilistic analysis of skewed highway bridges", *Struct. Eng. Mech.*, **55**(6), 1177-1202.

Bayat, M., Daneshjoo, F. and Nisticò, N. (2017a), "The effect of different intensity measures and earthquake directions on the seismic assessment of skewed highway bridges", *Earthq. Eng. Eng. Vib.*, **16**(1), 165-179.

Bayat, M., Daneshjoo, F., Nistico, N. and Pejovic, J. (2017b), "Seismic evaluation of isolated skewed bridges using fragility function methodology", *Comput. Concrete*, **20**(4), 419-427.

Bozorgnia, Y. and Bertero, V.V. (2004), *Earthquake Engineering: from Engineering Seismology to Performance-based Engineering*, CRC Press.

Burdette, N.J., Elnashai, A.S., Lupoi, A. and Sextos, A.G. (2008a), "Effect of asynchronous earthquake motion on complex bridges. I: Methodology and input motion", *J. Bridge Eng.*, **13**(2), 158-165.

Burdette, N.J., Elnashai, A.S., Lupoi, A. and Sextos, A.G. (2008b), "Effect of asynchronous earthquake motion on complex bridges. I: Methodology and input motion", *J. Bridge Eng.*, **13**(2), 158-165.

Caltrans, S.D.C. (2010), "Caltrans seismic design criteria version 1.6", California Department of Transportation, Sacramento, USA.

Chopra, A.K. (2016), *Dynamics of Structures: Theory and Applications to Earthquake Engineering*, 5th Edition, Prentice-hall International Series, USA.

Chou, C.C. and Chen, J.H. (2011), "Analytical model validation and influence of column bases for seismic responses of steel post-tensioned self-centering MRF systems", *Eng. Struct.*, **33**(9), 2628-2643.

Code, P. (2005), Eurocode 8: Design of Structures for Earthquake Resistance-Part 1: General Rules, Seismic Actions and Rules for Buildings, European Committee for Standardization, Brussels.

Council, B.S.S. (2000), FEMA 356-Prestandard and Commentary for the Seismic Rehabilitation of Buildings, Washington DC: Federal Emergency Management Agency, USA.

Desantiago, E., Mohammadi, J. and Albaijat, H.M. (2005), "Analysis of horizontally curved bridges using simple finite-element models", *Pract. Period. Struct. Des. Constr.*, **10**(1), 18-21.

Elnashai, A.S., Papanikolaou, V. and Lee, D.H. (2010), ZEUS-NL, University of Illinois at Urbana-Champaign, Mid-America Earthquake Center, USA.

Faal, H.N. and Poursha, M. (2017), "Applicability of the N2, extended N2 and modal pushover analysis methods for the seismic evaluation of base-isolated building frames with lead rubber bearings (LRBs)", *Soil Dyn. Earthq. Eng.*, **98**, 84-100.

Federal Emergency Management Agency (FEMA) (1997), NEHRP Guidelines for the Seismic Rehabilitation of Buildings, Report FEMA, 273, USA.

FEMA, F. (2007), 461-Interim Protocols for Determining Seismic Performance Characteristics of Structural and Nonstructural Components Through Laboratory Testing, Federal Emergency Management Agency (FEMA), Washington DC, USA.

Gidaris, I. and Taflanidis, A.A. (2013), "Parsimonious modeling of hysteretic structural response in earthquake engineering: Calibration/validation and implementation in probabilistic risk assessment", *Eng. Struct.*, **49**, 1017-1033.

Hashemi, A. and Loth, F. (2014), "Transition to turbulence in curved pipe", *APS Meeting Abstracts*, November.

Hashemi, A., Eshraghi, M. and Felicelli, S. (2015), "A three-dimensional multi-mesh lattice boltzmann model for multiphysics simulations", *APS Division of Fluid Dynamics Meeting Abstracts*, November.

Hashemi, A., Fischer, P.F. and Loth, F. (2018), "Direct numerical simulation of transitional flow in a finite length curved pipe", *J. Turbul.*, **19**(8), 664-682.

Jeon, J.S., Shafieezadeh, A., Lee, D.H., Choi, E. and DesRoches, R. (2015), “Damage assessment of older highway bridges subjected to three-dimensional ground motions: characterization of shear-axial force interaction on seismic fragilities”, *Eng. Struct.*, **87**, 47-57.
Kia, M., Banazadeh, M. and Bayat, M. (2018), “Rapid seismic vulnerability assessment by new regression-based demand and collapse models for steel moment frames”, *Earthq Struct.*, **14**(3), 203-214.
Krawinkler, H. (1992), “Guidelines for cyclic seismic testing of components of steel structures”, Applied Technology Council, Redwood City, Calif, USA.
Krawinkler, H. and Seneviratna, G.D.P.K. (1998), “Pros and cons of a pushover analysis of seismic performance evaluation”, *Eng. Struct.*, **20**(4-6), 452-464.
Luo, J., Fahnestock, L.A. and LaFave, J.M. (2017), “Nonlinear static pushover and eigenvalue modal analyses of quasi-isolated highway bridges with seat-type abutments”, *Struct.*, **12**, 145-167.
Mahdavi, N., Ahmadi, H.R. and Mahdavi, H. (2012), “A comparative study on conventional push-over analysis method and incremental dynamic analysis (IDA) approach”, *Sci. Res. Essay.*, **7**(7), 751-773.
Mander, J.B., Priestley, M.J. and Park, R. (1988), “Theoretical stress-strain model for confined concrete”, *J. Struct. Eng.*, **114**(8), 1804-1826.
Martínez-Rueda, J.E. and Elnashai, A.S. (1997), “Confined concrete model under cyclic load”, *Mater. Struct.*, **30**(3), 139-147.
Naghadehi, M.Z. and Mikaeil, R. (2017), “Optimization of tunnel boring machine (TBM) disc cutter spacing in jointed hard rock using a distinct element numerical simulation”, *Periodica Polytechnica Civil Eng.*, **61**(1), 56-65.
Naghadehi, M.Z., Benardos, A., Javdan, R., Tavakoli, H. and Rojhani, M. (2016), “The probabilistic time and cost risk analysis of a challenging part of an urban tunneling project”, *Tunnel. Underg. Space Technol.*, **58**, 11-29.
Naghadehi, M.Z., Jimenez, R., KhaloKakaie, R. and Jalali, S.M.E., (2011), “A probabilistic systems methodology to analyze the importance of factors affecting the stability of rock slopes”, *Eng. Geology*, **118**(3-4), 82-92.
Next Generation Attenuation of Ground Motions (Nga) Project (2006), http://Peer.Berkeley.Edu\nga\ (Accessed 10 October 2006)
Oinam, R.M., Sugumar, R. and Sahoo, D.R. (2017), “A comparative study of seismic performance of RC frames with masonry in fills”, *Procedia Eng.*, **173**, 1784-1791.
Panyakapo, P. (2014), “Cyclic pushover analysis procedure to estimate seismic demands for buildings”, *Eng. Struct.*, **66**, 10-23.
Purba, R. and Bruneau, M. (2015), “Experimental investigation of steel plate shear walls with in-span plastification along horizontal boundary elements”, *Eng. Struct.*, **97**, 68-79.
SEAOC (1995), Performance Based Seismic Engineering of Buildings, Structural Engineers Association of California, Sacramento, California, USA.
Sobhan, M.S., Rofooei, F.R. and Attari, N.K. (2017), “Buckling behavior of the anchored steel tanks under horizontal and vertical ground motions using static pushover and incremental dynamic analyses”, *Thin Wall. Struct.*, **112**, 173-183.
Vamvatsikos, D. and Cornell, C.A. (2002), “Incremental dynamic analysis”, *Earthq. Eng. Struct. Dyn.*, **31**(3), 491-514.
Vamvatsikos, D. and Cornell, C.A. (2004), “Applied incremental dynamic analysis”, *Earthq. Spectra*, **20**(2), 523-553.

CC